energies

MDPI

Article

Concepts for Hydrogen Internal Combustion Engines and Their Implications on the Exhaust Gas Aftertreatment System

Stefan Sterlepper [1,*], Marcus Fischer [1], Johannes Claßen [1], Verena Huth [2] and Stefan Pischinger [1]

[1] Thermodynamics of Energy Conversion Systems, RWTH Aachen University, 52074 Aachen, Germany; fischer_ma@tme.rwth-aachen.de (M.F.); classen_joh@tme.rwth-aachen.de (J.C.); Pischinger_s@tme.rwth-aachen.de (S.P.)
[2] FEV Europe GmbH, 52078 Aachen, Germany; huth_v@fev.com
* Correspondence: Sterlepper_s@tme.rwth-aachen.de; Tel.: +49-241-80-48055

Abstract: Hydrogen as carbon-free fuel is a very promising candidate for climate-neutral internal combustion engine operation. In comparison to other renewable fuels, hydrogen does obviously not produce CO_2 emissions. In this work, two concepts of hydrogen internal combustion engines (H_2-ICEs) are investigated experimentally. One approach is the modification of a state-of-the-art gasoline passenger car engine using hydrogen direct injection. It targets gasoline-like specific power output by mixture enrichment down to stoichiometric operation. Another approach is to use a heavy-duty diesel engine equipped with spark ignition and hydrogen port fuel injection. Here, a diesel-like indicated efficiency is targeted through constant lean-burn operation. The measurement results show that both approaches are applicable. For the gasoline engine-based concept, stoichiometric operation requires a three-way catalyst or a three-way NO_X storage catalyst as the primary exhaust gas aftertreatment system. For the diesel engine-based concept, state-of-the-art selective catalytic reduction (SCR) catalysts can be used to reduce the NOx emissions, provided the engine calibration ensures sufficient exhaust gas temperature levels. In conclusion, while H_2-ICEs present new challenges for the development of the exhaust gas aftertreatment systems, they are capable to realize zero-impact tailpipe emission operation.

Keywords: hydrogen; internal combustion engine; emissions; NOx; exhaust gas aftertreatment; $DeNO_X$; gaseous direct injection; port fuel injection; passenger cars; heavy duty vehicles

Citation: Sterlepper, S.; Fischer, M.; Claßen, J.; Huth, V.; Pischinger, S. Concepts for Hydrogen Internal Combustion Engines and Their Implications on the Exhaust Gas Aftertreatment System. *Energies* **2021**, *14*, 8166. https://doi.org/10.3390/en14238166

Academic Editors: Alessandro D'Adamo, Stefano Fontanesi and Giuseppe Cantore

Received: 17 October 2021
Accepted: 29 November 2021
Published: 6 December 2021

1. Introduction

Sustainability is the key driver for the transformation of powertrains for mobile and stationary solutions. It requires the reduction of both greenhouse gas emissions and pollutant emissions. In this regard, facing the mobility sector, internal combustion engines (ICE) need to compete with battery electric vehicles (BEVs) and fuel cell electric vehicles (FCEVs). Selected advantages of ICEs compared to BEVs and FCEVs are the robustness towards ambient conditions as well as fuel and air impurities, the low demand for rare earths and precious metals and the well-established development and production processes [1,2]. Air/hydrogen charges have ignition limits of $0.15 < \lambda < 10.5$ which are much wider than those of conventional fuels such as gasoline or diesel, enabling both operation principles. Furthermore, operation on hydrogen enables ICEs to reduce fuel-based carbon dioxide (CO_2) emissions down to zero. Lubrication oil-based CO_2 emissions are expected to be on a negligibly low level [3]. The latest research on combustion engines in general targets zero-impact tailpipe emissions [4]. The idea of zero-impact combustion engines are negligible tailpipe emissions, e.g., a pollutant contribution of traffic below a clean rural background. Addressing this challenge will bring down the propulsion system discussion from a political level to an efficiency-based, use-case specific evaluation.

Hydrogen internal combustion engines (H_2-ICE) have already been in development for some years [5–8]. In the early 2000s, BMW introduced their Hydrogen 7 as series

production vehicle [9,10]. It featured a modified gasoline V12 engine with 6 L displacement and hydrogen port fuel injection (PFI). A major drawback of the concept was the low specific load which resulted in a power output reduction from 327 kW at gasoline to 191 kW at hydrogen operation. Additionally, Ford [11,12] and others did extensive research and development work on H_2-ICEs [6]. Despite that, the hydrogen engine has not been able to establish itself. Recently, the hydrogen combustion engine has come back into focus in the automotive industry [13–17]. Specific loads at the level of gasoline or diesel engines are possible by using suitable boosting concepts [18]. A technology that is still under development and requires high research and development effort is the hydrogen direct injection (DI) [1,19,20]. One problem is that hydrogen has no lubricating properties, unlike conventional fuels [8]. This can lead to severe wear of the injectors and result in fast failure. Similar to CNG injectors, not the multi-hole but the A-nozzle injectors are expected to be the most reasonable solution. Another object of the research is the right hydrogen rail pressure [21]. On the one hand, high pressures are necessary to enable a rapid and late injection during the compression stroke. On the other hand, however, higher pressures reduce the effective tank capacity, which can only be used down to the level of the rail pressure. This leads to relatively early injection, possibly even with the intake valves still open, resulting in disadvantages similar to those of PFI. In the worst case, and favored by the wide ignition limits of hydrogen, backfiring occurs, where a hydrogen/air mixture ignites in the intake manifold. This poses a very high risk of causing damage to the engine.

Considering the exhaust composition, instead of CO_2, water is the main combustion product and is thus present in higher concentrations as in gasoline or diesel exhaust gas [3]. At $\lambda = 1$, the molar fraction of water is $\psi_{H2O} = 34\%$. Water vapor has a heat capacity of $c_{p,100\,°C} = 2.08$ kJ/(kg*K) increasing the overall heat capacity of the exhaust gases. Additionally, the high water content needs consideration regarding the impact on catalyst aging. The changed conditions for the operation of the exhaust gas aftertreatment system (ETAS) require the investigation of the system with regard to its complete service life [22].

Pollutant emissions are mainly nitrogen-based, with nitrogen oxide (NO_X) as the main raw emission. Potential secondary emissions produced in the exhaust aftertreatment system (EATS) are ammonia (NH_3) and nitrous oxide (N_2O), which, with the introduction of the EU7 legislation, are also expected to receive limit values that must be met in the real driving emissions type approval tests on the road [23–25]. Carbon-based pollutant emissions (carbon monoxide and hydrocarbons) can only result from lubrication oil consumption and are expected to be on a very low level.

NO_X aftertreatment ($DeNO_X$) systems from diesel engines can be adopted for lean operated hydrogen engines [26]. Such are either NO_X storage catalysts (NSC) or selective catalytic reduction (SCR) catalysts with additional injection of an aqueous urea solution. An additional technology for NO_X aftertreatment is the H_2-SCR, which utilizes hydrogen instead of the urea solution [27]. A big advantage is that no additional fluid needs integration and frequent refilling. Kureti et al. [28–30] and others [31,32] are investigating both Pt and Pd-based H_2-SCR catalysts and measure efficiencies of up to 95%. The H_2-SCR shows the best conversion performance roughly around ~150 °C, which is way below the light-off temperature of modern commercial technologies. Further development is needed to widen the currently very limited temperature operation range and to increase the nitrogen selectivity to prevent the conversion into N_2O.

In summary, there was intensive research and a lot of development activities in the past, but the H_2-ICE has just recently come back into focus. The characteristics of hydrogen as a fuel still results in various challenges and different, partly contradictory, solutions are possible. The objective of this work is to understand the main implications of the fundamental engine design on the exhaust gas aftertreatment system. For this purpose, exhaust gas parameters such as the relative air/fuel ratio, exhaust gas temperature and mass flow rate and NO_X concentration are investigated.

This paper presents measurement results from two recent experimental test campaigns with series production engines. Both engines are modified but not explicitly optimized or redesigned for hydrogen operation, leaving room for future progress. One of the two engines is based on a compressed natural gas (CNG)-fueled passenger car engine, once originally developed as a gasoline engine. The other one is based on a series production diesel engine that was previously modified for CNG operation. Both are presented in Figure 1 and will be referred to as gasoline and diesel engine-based concepts in the following.

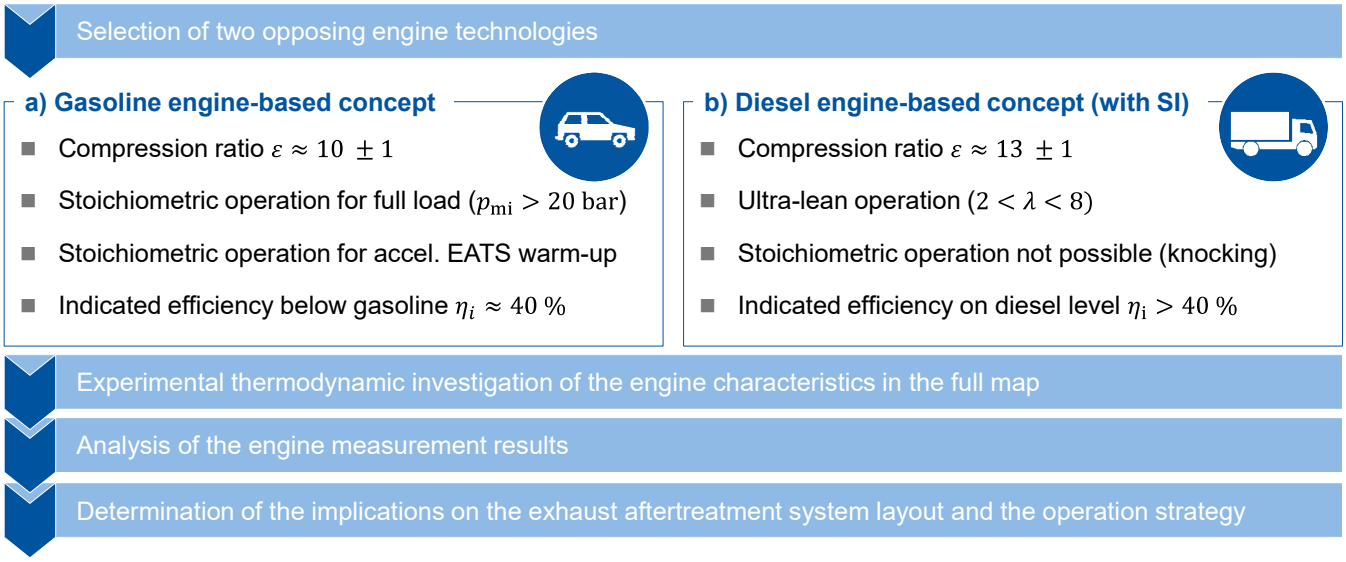

Figure 1. Experimental procedure of this investigation and introduction if the selected H_2-ICE concepts.

2. Materials and Methods

As explained above, an H_2-ICE can be equipped with PFI or DI. In both cases, knocking combustion can occur at high loads, early centers of combustion and low air/fuel ratios [33,34]. At the same time, enleanment improves the efficiency. As a result, the H_2-ICE features spark-ignition (SI), but enables quality control, which classifies it in between conventional gasoline and diesel concepts (Figure 1). In this work, representative engines of both concepts are investigated experimentally. The applied test procedure is also presented in Figure 1. Thermodynamic work packages will be introduced in separate publications. The present paper focuses on the impact of thermodynamic measurement results on the exhaust aftertreatment system.

The gasoline engine-based concept features a three-cylinder passenger car engine with a total displacement of 1 L. The cylinder charge motion is tumble supported and the CNG injectors of the base engine are modified with an external lubrication system for H_2 direct injection with 20 bar. To limit the occurrence of knocking combustion, the compression ratio was kept at the CNG engine reference of $\varepsilon \approx 10$, which is at the typical level of gasoline engines. This enables stoichiometric operation of the engine, which is necessary to achieve higher specific loads. In addition, the engine is equipped with a high-pressure exhaust gas recirculation (EGR) system. No further optimization was conducted, especially no replacement of the boosting system or of the charge motion support as defined by the shape of the intake ports or the piston. This enables a concept study, but not the optimum performance that would be possible with a completely optimized and redesigned engine.

The heavy duty (HD) diesel engine-based concept uses a modified six-cylinder engine with a total displacement of 7.8 L. It was modified from diesel to CNG operation beforehand by the implementation of spark plugs and PFI. To realize high mean effective pressures in a lean-burn operation, the single-stage turbocharging system was replaced by a two-stage turbocharger arrangement. The compression ratio of $\varepsilon = 13$ of the diesel engine was retained. This leads to severe knocking at low lambda values, which prohibits

stoichiometric operation [35]. At the same time, this compression ratio enables very lean operation up to λ = 8 and shows efficiencies that can compete with diesel engines.

Both engines were equipped with extensive emission analysis equipment. This includes an emissions analyzer from FEV containing a chemiluminescence detector (CLD), a paramagnetic detector (PMD), a nondispersive infrared sensor (NDIR) and flame ionization detector (FID) for measurements of NO_X, O_2, CO, CO_2 and HC emissions. Additionally equipped are a HSense from V&F for hydrogen measurements and a FTIR from MKS for H_2O and multiple other emissions.

3. Results

3.1. Gasoline Engine-Based Hydrogen Engine for Passenger Car Applications

The small three-cylinder passenger car hydrogen engine is intended to compete with the gasoline version in terms of power and maximum mean effective pressures. The hydrogen version was thus adapted for stoichiometric operation at full load. Here, the achievable mean effective pressure level is limited by the unchanged turbocharging system. In addition, the combustion chamber design is not optimized for mixture formation with hydrogen, causing mixture inhomogeneities. Despite the compression ratio of ε = 10, knocking occurs, which limits the usable range of the ignition timing at full load. To illustrate, where the engine is not operated as efficiency optimal to prevent from knocking, Figure 2 shows the point of 50% mass fraction burned (MFB50) in the engine map as indication for the center of combustion. The highest efficiency is achieved at MFB50 = 8 °CA_{aTDC} as a compromise between the constant volume process and wall heat losses. However, the ignition and accordingly also the MFB50 is retarded beyond 16 °CA_{aTDC} at loads above a brake mean effective pressure of BMEP = 16 bar.

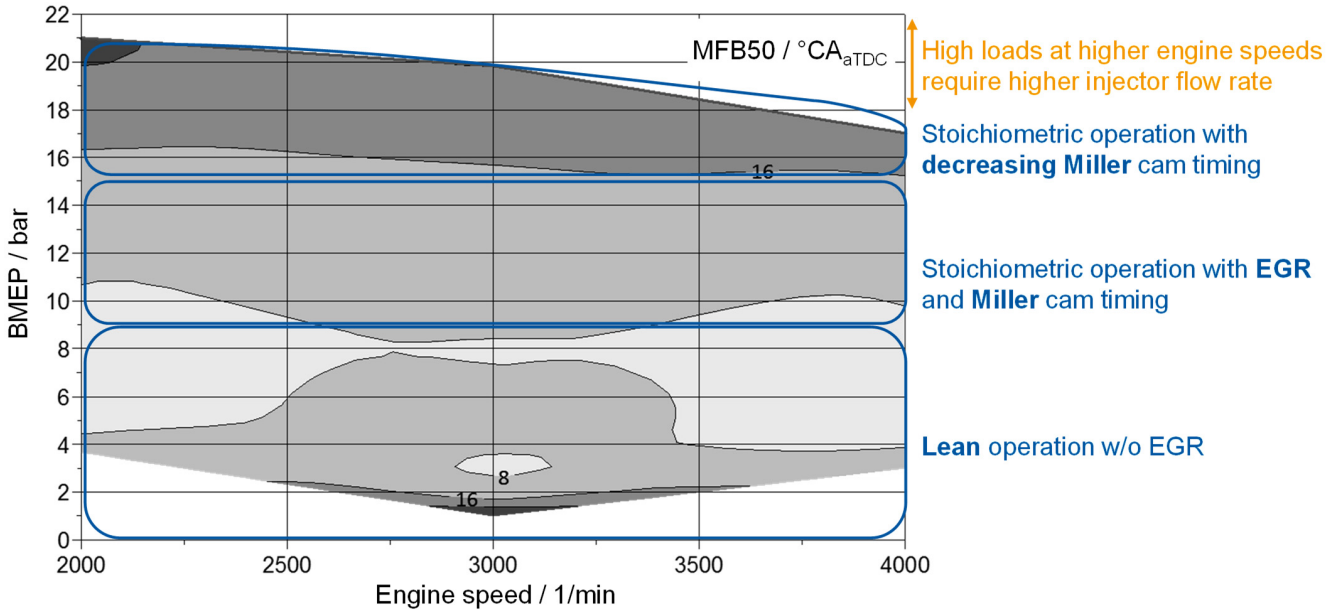

Figure 2. Engine operation strategy as result of previous thermodynamic investigations. The position of 50% fuel mass fraction burned (MFB50) shows an efficiency optimal operation for low and mediums loads, but a retarded combustion due to knocking at higher loads.

The operation strategy derived from thermodynamic investigations is presented in Figure 2. At full load, stoichiometric operation and a decreasing Miller timing is required to deliver the required cylinder charge. In the range of medium BMEPs, Miller timing and exhaust gas recirculation are favorable for de-throttling. In addition, the flame cooling effects of the EGR lead to a NO_X raw emission reduction [36]. In order to achieve maximum efficiency, the ignition angle is set for an MFB50 of approximately 8 °CA_{aTDC}, wherever

knocking allows. At low BMEPs, lean engine operation becomes more efficient than operation with EGR. The reason is a reduction in NO_X formation as can be seen in Figure 3.

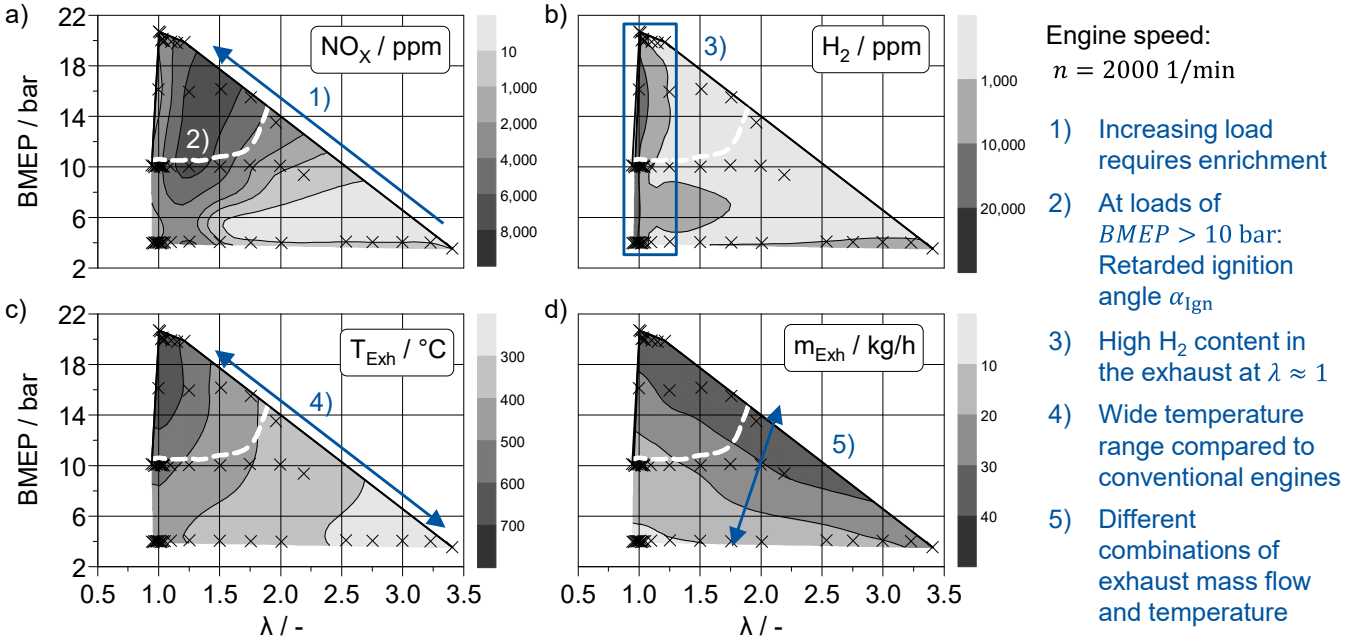

Figure 3. Characterization of the engine-out exhaust gas conditions as function of the air/fuel ratio λ: (**a**) Nitrogen oxide emissions, (**b**) Hydrogen content in the exhaust, (**c**) Exhaust gas temperature, (**d**) Exhaust gas mass flow. Measurement points at n = 2000 1/min are visualized as crosses. Measurements at other engine speeds also account into the interpolation, but as fourth dimension they cannot be displayed.

The graphs in Figure 3 show the reasonable BMEP ranges as a function of the air/fuel ratio. It can be seen that the area of BMEP narrows at higher loads towards stoichiometric conditions. The maximum air/fuel ratio is limited by the amount of air introduced into the cylinders and decreases with increasing fuel mass required for increasing load. Another boundary condition is shown by the white dashed line. It marks the range up to which an efficiency optimized MFB50 is applicable. At higher loads, the ignition angle α_{Ign} needs to be increased to prevent knocking.

In Figure 3a, the NO_X emissions are shown as a function of the relative air/fuel ratio and load. It can be seen that, starting at stoichiometric conditions, a minor enleanment leads to increased NO_X emissions, as known from gasoline engines. With more oxygen present in the exhaust gas, the NO_X formation tendency increases. After reaching a maximum around λ = 1.3, the NO_X emissions decrease significantly below the level of stoichiometric conditions.

This is a consequence of the decreasing temperature, as shown in Figure 3c. As a result, lean operation is beneficial in terms of NO_X emissions only at low loads. This is also the reason for splitting of the operation strategy into EGR for de-throttling at medium loads and enleanment at low loads (Figure 2). Looking at the unburned fraction of hydrogen in Figure 3b, significant H_2 emissions are detected around stoichiometric operation. These are attributed to the not optimized combustion chamber design. An optimized mixture formation and combustion process will significantly increase the indicated efficiency.

Additional important parameters for the exhaust gas aftertreatment system are temperature and mass flow of the exhaust gas. The exhaust gas temperature (Figure 3c) highly depends on the air/fuel ratio and varies in a wide range from below T_{Exh} = 300 °C to above T_{Exh} = 600 °C. The isolines of the exhaust mass flow in Figure 3d are vertical to the temperature isolines. This means that several combinations of temperatures and mass flows are possible, which is an additional degree of freedom for the EATS operation strategy in comparison to gasoline engines. In this regard, lower mass flows resulting in lower

space velocities and thus more reaction time are positive for the exhaust gas system at temperatures with slow reaction kinetics.

3.2. Diesel Engine-Based Hydrogen Engine for Heavy Duty Applications

A strongly different concept to the one shown in the chapter above is the diesel engine-based hydrogen engine. It combines a high compression ratio with hydrogen port fuel injection and a two-stage turbo charger arrangement. This leads to benefits in the operation efficiency. However, with this high compression ratio, stoichiometric operation is no longer possible. The knock limitation to lower lambda values ranges in between $1.5 \leq \lambda \leq 2$. The main exhaust gas parameters in the engine map of an efficiency oriented calibration is depicted in Figure 4.

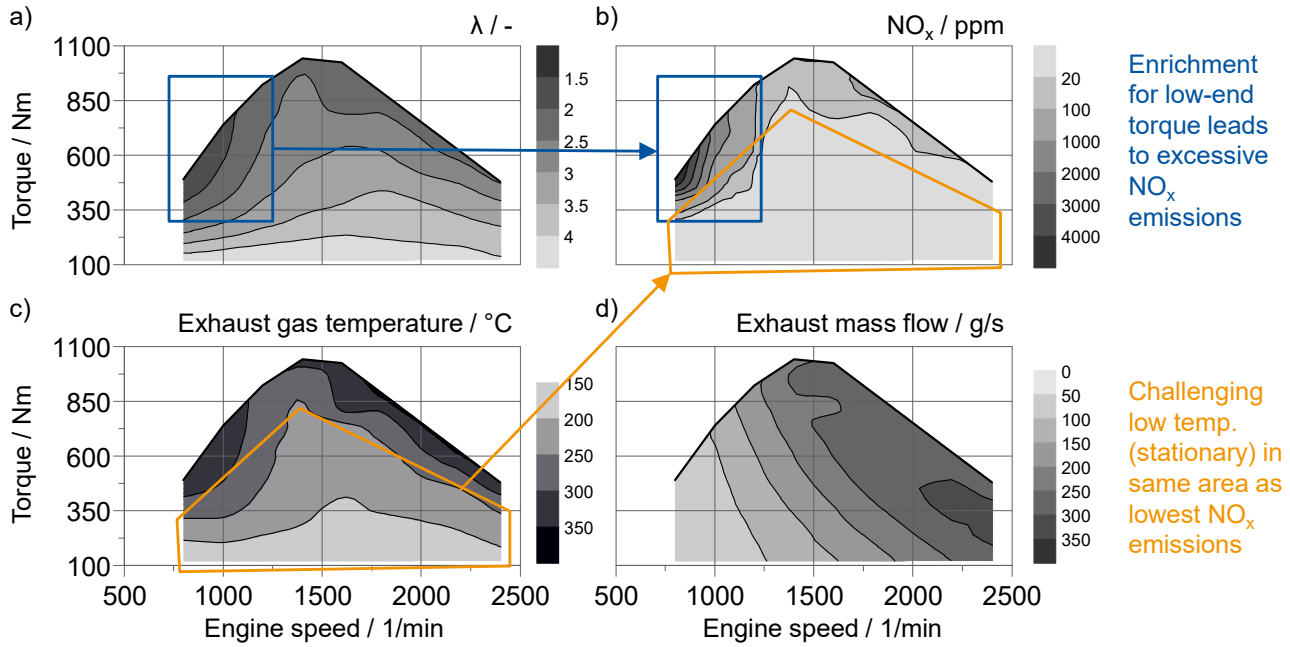

Figure 4. EATS boundary conditions with an efficiency orientated ultra-lean calibration: (**a**) Air-fuel ratio, (**b**) Nitrogen oxide emissions, (**c**) Exhaust gas temperature, (**d**) Exhaust gas mass flow. Here the load is expressed as engine torque.

In Figure 4a, the relative air/fuel ratio is plotted in the engine map as the function of engine speed and torque. The engine operates at lean conditions, close to the lean operation limit, where incomplete or instable combustion occurs. As noted for the gasoline engine-based concept in Figure 3, the lean operation limit decreases towards higher loads. The lean limit of stable operation under varying boundary conditions ranges from $\lambda > 4$ at low loads up to $\lambda < 2$ at the low-end torque. Moreover, also similar to the gasoline engine-based hydrogen engine in Figure 3, the exhaust temperatures in Figure 4c show a strong correlation to the air/fuel ratio. The lowest temperatures occur in ultra-lean operation at low load and even reach values below $T_{Exh} < 200$ °C. Even at high loads, the exhaust temperatures do not exceed $T_{Exh} = 350$ °C with this configuration.

As a result of this ultra-lean engine calibration, low cylinder temperatures and accordingly low exhaust gas temperatures apply (the latter depicted in Figure 4c). This results in low NO_X emissions measured in the raw exhaust gas. A wide area of more than three quarters of the map shows emissions of $\psi_{NOx} < 20$ ppm (lower marked area in Figure 4b). At engine speeds of $n > 1500$ 1/min, maximum NO_X emissions at full load are still limited to $\psi_{NOx} = 100$ ppm (upper area). Only the area of low-end torque shows severe NO_X emissions as a result of the comparably rich air/fuel ratio. However, the engine control functions and the calibration of the respective parameters were not yet finalized and a significant reduction towards more reasonable NO_X emissions can be expected. Again, the

exhaust mass flow isolines (Figure 4d) are more or less vertical to the temperature isolines. This challenges the EATS to perform under all possible combinations.

With the findings from above and additional thermodynamic investigations, it was found that for $\lambda > 2$, only very small advantages were observed in terms of the indicated efficiency. In a second development step, another calibration approach was applied. This time, the target is not at the highest indicated efficiency, but at moderate exhaust temperatures. The recalibration of the engine control functions focuses on the low speed and load ranges, which poses the greatest challenges for cold start and the subsequent warm-up phase. The resulting new engine maps are presented in Figure 5.

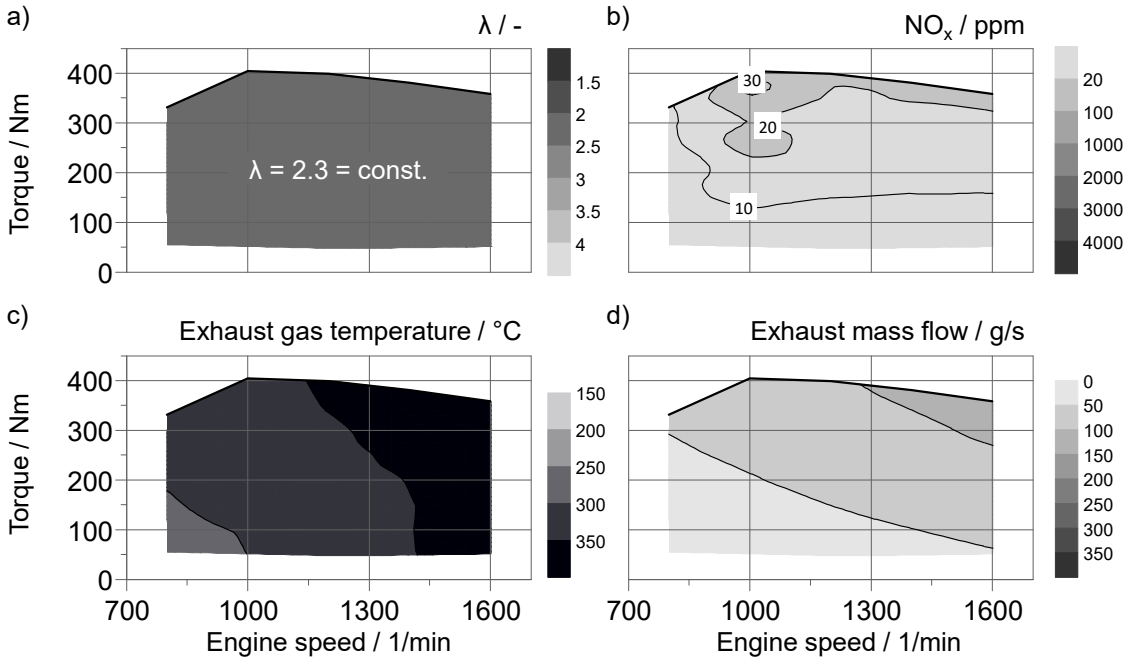

Figure 5. EATS boundary conditions under exhaust gas temperature-orientated lean operation: (**a**) Air-fuel ratio, (**b**) Nitrogen oxide emissions, (**c**) Exhaust gas temperature, (**d**) Exhaust gas mass flow. The color bars are similar to those in Figure 4 in order to ensure the comparability.

The new engine control strategy targets an exhaust gas temperature above 250 °C as it is needed for conventional SCR systems. Therefore, lambda is decreased to $\lambda = 2.3$ as shown in Figure 5a. By this measure, the exhaust temperature increases above 300 °C in the whole map except for a very small area. This shows the strong impact of the engine calibration on the exhaust gas characteristics.

As discussed before, NO_X emissions are highly sensitive to changes in the relative air/fuel ratio. However, similar to the gasoline engine-based concept depicted in Figure 3a, at the relative air/fuel ratio of $\lambda = 2.3$, the NO_X reduction due to a dilution induced exhaust gas temperature dominates over the effect of an oxygen availability-induced NO_X increase. Thus, the positive effect of enleanment is achieved and the NO_X emissions are significantly below those of stoichiometric operation. Figure 5b shows NO_X emissions in the range of 30 ppm and below.

As an aside, it should be mentioned that the exhaust gas mass flow decreases slightly due to the reduced air mass flow with less enleanment (Figure 5d). Accordingly, in terms of absolute emissions (in g/kWh) and assuming a constant NO_X concentration, the reduction in exhaust mass flow leads to a corresponding reduction in NO_X emissions. In other words, the mass flow reduction already contributes to a slight increase in NO_X concentration without producing more NO_X in absolute terms.

4. Discussion

The results of both measurement campaigns depict very different exhaust gas characteristics. The gasoline engine-based H_2-ICE with a low compression ratio and small displacement causes rather high NO_X raw emissions at higher loads, but also high exhaust gas temperatures. On the contrary, the diesel engine-based H_2-ICE with a higher compression ratio and two-stage turbocharging emits NO_X raw emissions on a very low level. This is achieved by further enleanment, which leads to lowered exhaust gas temperatures.

Considering suitable exhaust gas aftertreatment systems, the determining factor is the stoichiometric operation of the gasoline engine-based hydrogen engine at higher loads. Stoichiometric operation is necessary to achieve the desired specific loads of up to BMEP > 20 bar, where the air charge is limited by the series production boosting system of the gasoline engine. At stoichiometric operation, however, an optimization of the mixture formation towards nearly complete combustion leads to very low oxygen concentrations. Under these stoichiometric conditions, conventional $DeNO_X$ systems such as an SCR or NO_X storage catalysts are not applicable. Instead, a three-way catalyst (TWC) is necessary for exhaust gas aftertreatment.

In contrast to gasoline engines, the exhaust gases contain no or only negligible carbon-based emissions. Thus, the TWC lacks CO or hydrocarbons as reducing agents that react with oxygen from the Ceroxide or convert stored NOx in the Barium oxide phase to nitrogen [37]. This role must be taken over by hydrogen. Appropriate references can be found in the literature [33,38]. However, hydrogen as reductant could lead to new TWC material formulations in the future and will remain an object of research [39].

When switching between stoichiometric and lean operation, another subject is the TWC performance under lean conditions. Krishnan Unni et al. [40] operated a H_2-ICE equipped with a TWC at lean conditions and still observed catalytic effects. With the full and thus practically deactivated oxygen storage, the catalytic effects can be attributed to the platinum group metals (PGM) acting as an oxidation catalyst (OC). This enables the TWC to replace an oxidation catalyst (OC) and provide NO_2 to a downstream SRC system, which requires an NO_2/NO_X ratio of about 1/2 to operate efficiently, depending on the material [41]. Accordingly, the aftertreatment concept for lean conditions could include a TWC and a SCR system. At that temperature level, a NH_3-SCR system is more sensible than an H_2-SCR. The NH_3-SCR might even operate as passive concept fed by secondary ammonia emissions of the TWC.

Another option for the exhaust gas aftertreatment is the three-way NO_X storage catalyst (TWNSC). It is capable of NO_X conversion under stoichiometric conditions but has a strongly increased NO_X storage capacity [42,43]. With this, the TWNSC is also applicable for lean operation, where it stores the NO_X. For the regeneration, cyclic rich operation is required. Alike the TWC, hydrogen as the only reducing agent leads to changed boundary conditions, posing similar material development challenges.

From this discussion, the EATS concepts for gasoline engine-based H_2-ICEs, including stoichiometric operation, shown in Figure 6a, emerge. Due to the stoichiometric operation of the gasoline engine-based concept, the introduction of a TWC or TWNSC is mandatory. However, for lean operation it needs to be supported by an additional $DeNO_X$ system, which is here an SCR catalyst as discussed beforehand.

Furthermore, Figure 6b introduces exhaust aftertreatment systems for the diesel engine-based concept. Here, lean engine operation enables low NO_X raw emissions. The aftertreatment concept is mainly depending on the exhaust gas temperature. Due to the favorable burn characteristics of hydrogen, a wide calibration range is possible [44]. Two scenarios based on the same diesel engine-based hydrogen engine are illustrated in Figures 4 and 5.

An engine calibration of the whole map at, e.g., $\lambda = 2.3$ enables exhaust gas temperatures high enough for SCR systems. The central aftertreatment component for lean engine concepts will be a selective catalytic reduction (SCR) catalyst, most likely combined with

some kind of oxidation catalyst upstream. One option with oxidizing characteristics under lean conditions is a NO_X storage catalyst (NSC).

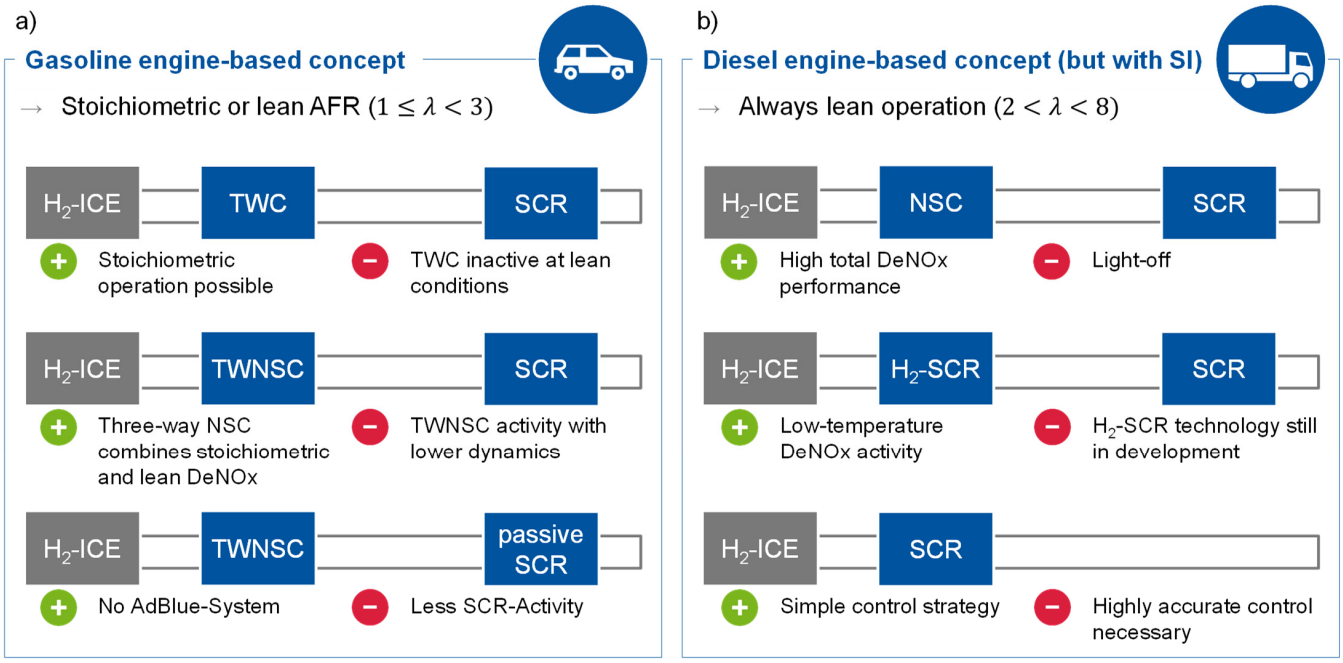

Figure 6. Aftertreatment system layout for (**a**) the gasoline engine-based concept including stoichiometric operation and (**b**) the HD diesel engine-based concept at always lean conditions.

The NSC could support the SCR to increase the overall conversion efficiency and is divided into two types: either lean NO_X traps (LNTs), which require rich conditions for regeneration phases, or passive NO_X adsorbers (PNAs), which release the NO_X at higher temperatures. Especially PNAs can also cover slightly lower exhaust gas temperatures and extend the EATS operation range.

As an alternative solution to the λ = 2.3 calibration, at ultra-lean operation almost no NO_X emissions are present and operation without exhaust gas aftertreatment is theoretically possible. However, transient operation scenarios lead to dynamic NO_X emission peaks that are not compliant without any EATS. At the same time, heavy enleanment leads to significantly lower exhaust gas temperatures below the light-off temperatures of conventional $DeNO_X$ systems, causing the EATS to be inactive.

Especially during the heat-up phase after a cold start, the low exhaust gas temperatures are challenging. A solution could be the application of an H_2-SCR system which has the highest efficiency at low temperatures. Installing it in first close-coupled position enables an early light-off even at extremely low exhaust gas temperatures. At higher temperatures, it could work as oxidation catalyst to form NO_2 for the SCR, as discussed before with the TWC. However, the H_2-SCR technology is still under development. As a result, all three EATS concepts in Figure 6b are most promising for the diesel engine-based H_2-ICE. The final decision will then be depending on the engine application.

In summary, the engine operation concept and the exhaust gas aftertreatment concept must be developed in parallel. A matching process is enabled by choosing the engine control strategy with respect to the requirements of the EATS. The NO_X raw emissions and the exhaust gas temperature are the dominating parameters. Compared to gasoline or diesel engines, the presence of hydrogen in the raw exhaust gas, high water fractions relative to the air/fuel ratio, and the absence of carbon-based emissions lead to new boundary conditions. Accordingly, the concepts developed for switching (between stoichiometric and lean) operation and permanent lean operation must face the same challenges, although they follow two contradictory approaches. As a result for both strategies, the potential

trade-off between low NO_X raw emissions and high catalytic conversion efficiency requires compromises that are specifically designed for the target application. With regard to future emission legislations, the environmentally friendly zero-impact tailpipe emissions include ultra-low emissions of N_2O and NH_3. This requires very precise ammonia dosing strategies that also consider passive NH_3 formation provided by upstream catalysts (TWC, TWNSC or NSC). As an alternative, additional ammonia slip catalysts could be integrated. However, the oxidizing characteristics of ammonia slip catalysts (ASC) may increase the N_2O emissions. For that reason, ASCs were not considered in the suggested concepts within Figure 6.

Finally, the previously discussed catalysts can also be combined on coated particulate filters, which could be considered due the potential of particulate formation resulting from combustion of lubrication oil [45]. The resulting ash accumulation is known to increase the filtration efficiency but may need further investigation due to the absence of fuel-induced soot particulates [46].

As a final remark, naming the two approaches gasoline engine- and diesel engine-based concepts is not intended to limit the applicable use range. These labels were chosen to describe their origin and some basic engine parameters such as compression ratio and displacement. Future solutions will be based on one of the concepts or something in between, considering the specific use-case and the performance priorities such as maximum efficiency, high specific load, low production costs or others. Additionally, both engines were not optimized for hydrogen operation with dedicated mixture formation or boosting strategies. This leaves further potential for future H_2-ICEs.

5. Conclusions

The conversion of internal combustion engines shows that contrary approaches are feasible, e.g., with different compression ratios enabling different operating strategies. Depending on the chosen approach, the following implications on the exhaust gas aftertreatment systems (EATS) apply.

For the gasoline engine-based hydrogen combustion engine with lower compression ratio (here $\varepsilon = 10$) aiming at high specific power, the following conclusions are drawn:

1. Lean operation is limited by the boosting system. Highest specific power is reached with stoichiometric combustion, which is accompanied by relatively high NO_X emissions. Thus, the EATS has to include either a three-way catalyst (TWC) or a three-way NO_X storage catalyst (TWNSC);
2. At low loads, lean operation is still more efficient. Here, we see an SCR catalyst as the system of choice. Under these conditions, the upstream TWC/TWNSC can be used as oxidation catalyst to increase the NO_2/NO_X ratio. If hydrogen is available in the exhaust, the TWC/TWNSC will also produce ammonia, which reduces the required amount of urea injection;
3. Switching between stoichiometric and lean operation will require dedicated engine operation strategies. Here, the avoidance of NO_X, NH_3 and N_2O emissions will most likely require high attention. Main conclusions for the diesel engine-based hydrogen combustion engine with higher compression ratio (here $\varepsilon = 13$) targeting high efficiency are the following:
4. Ultra-lean operation enables ultra-low NO_X raw emissions down to the limit of detectability. However, the heavy enleanment comes along with very low exhaust gas temperatures that are below the light-off temperatures of currently available catalysts. As a result, the exhaust gas aftertreatment system is not instantly available in the event of a transient operating point change;
5. From the exhaust gas aftertreatment point of view, less lean operation is beneficial. An engine operation, e.g., at an air/fuel ratio of $\lambda = 2.3$ still causes low NO_X emissions, but increases the exhaust temperature to ensure catalyst activity;
6. Under these operation conditions, the SCR catalyst is the most promising EATS component and can be directly transferred from diesel applications. For operation

areas, where the SCR system is not fully active, a combination with an upstream NO_X storage catalyst or H_2-SCR system increases the overall NO_X reduction performance.

In summary, the exhaust aftertreatment systems have to focus on nitrogen related emissions: NO_X as primary and NH_3 and N_2O as secondary emission species. Engine operation with decreasing exhaust temperatures challenges the exhaust gas aftertreatment system. The trade-off between NO_X raw emission reduction and catalyst conversion efficiency losses requires application-specific investigations to achieve the lowest tailpipe emissions.

Finally, the hydrogen combustion engine will be capable of achieving zero-impact tailpipe emissions. The according exhaust gas aftertreatment systems may be less complex than such for gasoline or diesel applications with similarly low tailpipe emission levels. However, for that, the engine and exhaust aftertreatment layout as well as engine and aftertreatment operation strategies have to be closely aligned. Additionally, further research on catalyst materials, operation strategies and degradation mechanisms is necessary.

Author Contributions: Conceptualization, S.S. and J.C.; validation and formal analysis, S.S., M.F., V.H. and J.C.; investigation, S.S., M.F. and V.H.; resources, M.F. and V.H.; data curation, M.F. and V.H.; writing—original draft preparation, S.S.; writing—review and editing, S.S., M.F., J.C., V.H. and S.P.; visualization, S.S.; supervision, S.P. All authors have read and agreed to the published version of the manuscript.

Funding: The presented research work was carried out at the Center for Mobile Propulsion (CMP) of RWTH Aachen University with funding by the German Science Council Wissenschaftsrat (WR) and the German Research Foundation Deutsche Forschungsgemeinschaft (DFG).

Acknowledgments: The authors would like to thank Ford Werke GmbH for providing the passenger car engine and accompanying advice, and FEV Europe GmbH for providing the heavy-duty engine and advice on both engines.

Conflicts of Interest: The authors declare no conflict of interest.

References

1. Verhelst, S. Recent progress in the use of hydrogen as a fuel for internal combustion engines. *Int. J. Hydrogen Energy* **2014**, *39*, 1071–1085. [CrossRef]
2. Candelaresi, D.; Valente, A.; Iribarren, D.; Dufour, J.; Spazzafumo, G. Comparative life cycle assessment of hydrogen-fuelled passenger cars. *Int. J. Hydrogen Energy* **2021**, *46*, 35961–35973. [CrossRef]
3. Ma, D.-S.; Sun, Z.Y. Progress on the studies about NOx emission in PFI-H2ICE. *Int. J. Hydrogen Energy* **2020**, *45*, 10580–10591. [CrossRef]
4. Thewes, M.; Balazs, A.; Yadla, S.K.; Walter, V.; Görgen, M.; Scharf, J.; Sterlepper, S.; Voßhall, T. Zero-Impact Combustion Engine. In Proceedings of the 28th Aachen Colloquium Automobile and Engine Technology, Aachen, Germany, 7–9 October 2019.
5. Nagalingam, B.; Dübel, M.; Schmillen, K. Performance of the Supercharged Spark Ignition Hydrogen Engine. *SAE Tech. Pap. Ser.* **1983**, 831688. [CrossRef]
6. Verhelst, S.; Wallner, T. Hydrogen-fueled internal combustion engines. *Prog. Energy Combust. Sci.* **2009**, *35*, 490–527. [CrossRef]
7. Eichlseder, H.; Wallner, T.; Freymann, R.; Ringler, J. The Potential of Hydrogen Internal Combustion Engines in a Future Mobility Scenario. *SAE Tech. Pap. Ser.* **2003**, 2003-01-2267. [CrossRef]
8. Yamane, K. Hydrogen Fueled ICE, Successfully Overcoming Challenges through High Pressure Direct Injection Technologies: 40 Years of Japanese Hydrogen ICE Research and Development. *SAE Tech. Pap. Ser.* **2018**, 2018-01-1145. [CrossRef]
9. Kiesgen, G.; Klüting, M.; Bock, C.; Fischer, H. The New 12-Cylinder Hydrogen Engine in the 7 Series: The H2 ICE Age Has Begun. *SAE Tech. Pap. Ser.* **2006**, 2006-01-0431. [CrossRef]
10. Wallner, T.; Lohse-Busch, H.; Gurski, S.; Duoba, M.; Thiel, W.; Martin, D.; Korn, T. Fuel economy and emissions evaluation of BMW Hydrogen 7 Mono-Fuel demonstration vehicles. *Int. J. Hydrogen Energy* **2008**, *33*, 7607–7618. [CrossRef]
11. Stockhausen, W.F.; Natkin, R.J.; Kabat, D.M.; Reams, L.; Tang, X.; Hashemi, S.; Szwabowski, S.J.; Zanardelli, V.P. Ford P2000 Hydrogen Engine Design and Vehicle Development Program. *SAE Tech. Pap. Ser.* **2002**, 2002-01-0240. [CrossRef]
12. Natkin, R.J.; Denlinger, A.R.; Younkins, M.A.; Weimer, A.Z.; Hashemi, S.; Vaught, A.T. Ford 6.8L Hydrogen IC Engine for the E-450 Shuttle Van. *SAE Tech. Pap. Ser.* **2007**, 2007-01-4096. [CrossRef]
13. Virnich, L.; Lindemann, B.; Müther, M.; Schaub, J.; Huth, V.; Geiger, J. How to Improve Transient Engine Performance of HD Hydrogen Engines while Maintaining Lowest NOx Emissions. In Proceedings of the 42th International Vienna Motor Symposium, Vienna, Austria, 28–30 April 2021; ISBN 978-3-9504969-0-1.

14. Pauer, T.; Weller, H.; Schünemann, E.; Eichlseder, H.; Grabner, P.; Schaffer, K. H2ICE for Future Passenger Cars and Light Commercial Vehicles. In Proceedings of the 41th International Vienna Motor Symposium, Vienna, Austria, 22–24 April 2020; ISBN 978-3-18-381312-4.
15. Dreisbach, R.; Arnberger, A.; Zukancic, A.; Wieser, M.; Kunder, N.; Plettenberg, M.; Raser, B.; Eichlseder, H. The Heavy-Duty Hydrogen Engine and its Realization until 2025. In Proceedings of the 42th International Vienna Motor Symposium, Vienna, Austria, 28–30 April 2021; ISBN 978-3-9504969-0-1.
16. Korn, T.; Nobile, R.-F.; Grassinger, D. Zero-Emission, Maximum Performance—The Latest Generation of Hydrogen Combustion Engines. In Proceedings of the 42th International Vienna Motor Symposium, Vienna, Austria, 28–30 April 2021; ISBN 978-3-9504969-0-1.
17. Walter, L.; Sommermann, A.; Hyna, D.; Malischewski, T.; Leistner, M.; Hinrichsen, F.; Wöhner, P.; Schmitt, J.; McMackin, M. The H2 Combustion Engine—The Forerunner of a Zero Emissions Future. In Proceedings of the 42th International Vienna Motor Symposium, Vienna, Austria, 28–30 April 2021; ISBN 978-3-9504969-0-1.
18. Wang, X.; Sun, B.; Luo, Q. Energy and exergy analysis of a turbocharged hydrogen internal combustion engine. *Int. J. Hydrogen Energy* **2019**, *44*, 5551–5563. [CrossRef]
19. Li, Y.; Gao, W.; Zhang, P.; Ye, Y.; Wei, Z. Effects study of injection strategies on hydrogen-air formation and performance of hydrogen direct injection internal combustion engine. *Int. J. Hydrogen Energy* **2019**, *44*, 26000–26011. [CrossRef]
20. Yip, H.L.; Srna, A.; Liu, X.; Kook, S.; Hawkes, E.R.; Chan, Q.N. Visualization of hydrogen jet evolution and combustion under simulated direct-injection compression-ignition engine conditions. *Int. J. Hydrogen Energy* **2020**, *45*, 32562–32578. [CrossRef]
21. Yip, H.L.; Srna, A.; Yuen, A.C.Y.; Kook, S.; Taylor, R.A.; Yeoh, G.H.; Medwell, P.R.; Chan, Q.N. A Review of Hydrogen Direct Injection for Internal Combustion Engines: Towards Carbon-Free Combustion. *Appl. Sci.* **2019**, *9*, 4842. [CrossRef]
22. Sterlepper, S.; Claßen, J.; Pischinger, S.; Görgen, M.; Cox, J.; Nijs, M.; Scharf, J. Relevance of Exhaust Aftertreatment System Degradation for EU7 Gasoline Engine Applications. *SAE Tech. Pap. Ser.* **2020**, 2020-01-0382. [CrossRef]
23. Wunsch, R.; Schön, C.; Frey, M.; Tran, D.; Proske, S.; Wandrey, T.; Kalogirou, M.; Schäffner, J. Detailed experimental investigation of the NOx reaction pathways of three-way catalysts with focus on intermediate reactions of NH3 and N2O. *Appl. Catal. B* **2020**, *272*, 118937. [CrossRef]
24. Claßen, J.; Pischinger, S.; Krysmon, S.; Sterlepper, S.; Dorscheidt, F.; Doucet, M.; Reuber, C.; Görgen, M.; Scharf, J.; Nijs, M.; et al. Statistically supported real driving emission calibration: Using cycle generation to provide vehicle-specific and statistically representative test scenarios for Euro 7. *Int. J. Engine Res.* **2020**, *21*, 1783–1799. [CrossRef]
25. Claßen, J.; Krysmon, S.; Dorscheidt, F.; Sterlepper, S.; Pischinger, S. Real Driving Emission Calibration—Review of Current Validation Methods against the Background of Future Emission Legislation. *Appl. Sci.* **2021**, *11*, 5429. [CrossRef]
26. Kawamura, A.; Yanai, T.; Sato, Y.; Naganuma, K.; Yamane, K.; Takagi, Y. Summary and Progress of the Hydrogen ICE Truck Development Project. *SAE Int. J. Commer. Veh.* **2009**, *2*, 110–117. [CrossRef]
27. Savva, P.G.; Costa, C.N. Hydrogen Lean-DeNOx as an Alternative to the Ammonia and Hydrocarbon Selective Catalytic Reduction (SCR). *Catal. Rev.* **2011**, *53*, 91–151. [CrossRef]
28. Leicht, M.; Schott, F.J.; Bruns, M.; Kureti, S. NOx reduction by H2 on WOx/ZrO2-supported Pd catalysts under lean conditions. *Appl. Catal. B* **2012**, *117–118*, 275–282. [CrossRef]
29. Hahn, C.; Endisch, M.; Schott, F.J.; Kureti, S. Kinetic modelling of the NOx reduction by H2 on Pt/WO3/ZrO2 catalyst in excess of O2. *Appl. Catal. B* **2015**, *168–169*, 429–440. [CrossRef]
30. Schott, F.J.P.; Balle, P.; Adler, J.; Kureti, S. Reduction of NOx by H2 on Pt/WO3/ZrO2 catalysts in oxygen-rich exhaust. *Appl. Catal. B* **2009**, *87*, 18–29. [CrossRef]
31. Olympiou, G.G.; Efstathiou, A.M. Industrial NOx control via H2-SCR on a novel supported-Pt nanocatalyst. *Chem. Eng. J.* **2011**, *170*, 423–432. [CrossRef]
32. Hamada, H.; Haneda, M. A review of selective catalytic reduction of nitrogen oxides with hydrogen and carbon monoxide. *Appl. Catal. A* **2012**, *421–422*, 1–13. [CrossRef]
33. Luo, Q.; Hu, J.-B.; Sun, B.; Liu, F.; Wang, X.; Li, C.; Bao, L. Effect of equivalence ratios on the power, combustion stability and NOx controlling strategy for the turbocharged hydrogen engine at low engine speeds. *Int. J. Hydrogen Energy* **2019**, *44*, 17095–17102. [CrossRef]
34. Lee, J.; Park, C.; Bae, J.; Kim, Y.; Choi, Y.; Lim, B. Effect of different excess air ratio values and spark advance timing on combustion and emission characteristics of hydrogen-fueled spark ignition engine. *Int. J. Hydrogen Energy* **2019**, *44*, 25021–25030. [CrossRef]
35. Li, Y.; Gao, W.; Zhang, P.; Fu, Z.; Cao, X. Influence of the equivalence ratio on the knock and performance of a hydrogen direct injection internal combustion engine under different compression ratios. *Int. J. Hydrogen Energy* **2021**, *46*, 11982–11993. [CrossRef]
36. Zhu, H.; Duan, J. Research on emission characteristics of hydrogen fuel internal combustion engine based on more detailed mechanism. *Int. J. Hydrogen Energy* **2019**, *44*, 5592–5598. [CrossRef]
37. Abdulhamid, H.; Fridell, E.; Skoglundh, M. Influence of the Type of Reducing Agent (H2, CO, C3H6 and C3H8) on the Reduction of Stored NOX in a Pt/BaO/Al2O3 Model Catalyst. *Top. Catal.* **2004**, *30–31*, 161–168. [CrossRef]
38. Ling-zhi, B.; Bai-gang, S.; Qing-he, L.; Yong-li, G.; Xi, W.; Fu-shui, L.; Chao, L. Simulation and experimental study of the NOx reduction by unburned H2 in TWC for a hydrogen engine. *Int. J. Hydrogen Energy* **2020**, *45*, 20491–20500. [CrossRef]
39. Lindholm, A.; Currier, N.; Fridell, E.; Yezerets, A.; Olsson, L. NOx storage and reduction over Pt based catalysts with hydrogen as the reducing agentInfluence of H2O and CO2. *Appl. Catal. B* **2007**, *75*, 78–87. [CrossRef]

40. Krishnan Unni, J.; Bhatia, D.; Dutta, V.; Das, L.M.; Jilakara, S.; Subash, G.P. Development of Hydrogen Fuelled Low NOx Engine with Exhaust Gas Recirculation and Exhaust after Treatment. *SAE Tech. Pap. Ser.* **2017**, 2017-26-0074. [CrossRef]
41. Schmieg, S.J.; Lee, J.-H. Evaluation of Supplier Catalyst Formulations for the Selective Catalytic Reduction of NOx With Ammonia. *SAE Tech. Pap. Ser.* **2005**, 2005-01-3881. [CrossRef]
42. Malamis, S.A.; Li, M.; Epling, W.S.; Harold, M.P. Steady state and lean-rich cycling study of a three-way NOX storage catalyst: Experiments. *Appl. Catal. B* **2018**, *237*, 588–602. [CrossRef]
43. Li, M.; Malamis, S.A.; Epling, W.; Harold, M.P. Steady state and lean-rich cycling study of a three-way NOX storage catalyst: Modeling. *Appl. Catal. B* **2019**, *242*, 469–484. [CrossRef]
44. Klell, M.; Eichlseder, H.; Sartory, M. Mixtures of hydrogen and methane in the internal combustion engine—Synergies, potential and regulations. *Int. J. Hydrogen Energy* **2012**, *37*, 11531–11540. [CrossRef]
45. Singh, A.P.; Pal, A.; Agarwal, A.K. Comparative particulate characteristics of hydrogen, CNG, HCNG, gasoline and diesel fueled engines. *Fuel* **2016**, *185*, 491–499. [CrossRef]
46. Sterlepper, S.; Claßen, J.; Pischinger, S.; Schernus, C.; Görgen, M.; Cox, J.; Nijs, M.; Scharf, J.; Rose, D.; Boger, T. Analysis of the Emission Conversion Performance of Gasoline Particulate Filters Over Lifetime. *SAE Int. J. Adv. Curr. Prac. Mobil.* **2020**, *2*, 710–720. [CrossRef]